

Empirical Correlations between ^{207}Pb NMR Chemical Shifts and Structure in Solids

F. Fayon,* I. Farnan,[†] C. Bessada, J. Coutures, D. Massiot, and J. P. Coutures

Contribution from the Centre de Recherche sur la Physique des Hautes Température—CNRS, 1D, Av. de la Recherche Scientifique, 45071 Orléans Cedex 2, France

Received October 15, 1996. Revised Manuscript Received May 8, 1997[⊗]

Abstract: Using ^{207}Pb magic angle spinning and static NMR, we have resolved and assigned different lead sites in crystalline lead oxides and lead silicates to their isotropic chemical shifts. Chemical shift anisotropies were also obtained for lead sites from the intensities of spinning sidebands. Empirical correlations between ^{207}Pb isotropic chemical shifts and structural parameters are proposed. For ionic compounds, we show good correlations between chemical shift and coordination number or mean bond length. For more covalent compounds, the best empirical correlation has been obtained by using the degree of oxygen s–p hybridization and second neighbor electronegativity similar to that previously used to characterize ^{29}Si shifts in aluminosilicates. The Pb^{2+} chemical shift anisotropies increase with more positive chemical shifts. These correlations, established for simple crystalline compounds, should allow better characterization of lead environments in disordered materials of complex composition.

Introduction

Lead contamination of the environment is a significant health hazard. A knowledge of the nature of lead speciation in waste disposal media is essential if we want to evaluate the long-term stability or resistance to external attack of those media. As waste disposal forms are often disordered materials of complex composition then an element-specific spectroscopic technique is preferred to give direct information on the local bonding environment of lead at the point of incorporation into the waste disposal medium. High-resolution solid-state nuclear magnetic resonance (NMR) has proved to be a powerful tool for the investigation of structure and local bonding in solids. However, interpretation of NMR chemical shift data requires a knowledge of the structure–shift relationship to be established empirically since the calculations of chemical shifts from electronic structure do not approach the precision to which they can be measured. In terms of nuclear spin ($I = 1/2$), gyromagnetic ratio, and natural abundance, ^{207}Pb would appear to be an attractive nucleus for the NMR spectroscopist. It has a slightly higher resonance frequency than ^{29}Si , the same spin, and a natural isotopic abundance almost five times greater. However, lead's large number of electrons, and hence polarizability, mean that even slight deviations from spherical symmetry lead to significant chemical shift anisotropies,¹ that can broaden the static resonance lines by more than 2000 ppm and chemical shifts have been reported to range over 7000–8000 ppm.^{1,2} This results in magic angle spinning (MAS) spectra with a large array of sidebands, even with spinning speeds of 15 kHz, that can be difficult to phase and to determine isotropic bands unambiguously. Here we present a series of detailed experiments that provide isotropic chemical shift data for a series of lead compounds. We attempt to provide an understanding of the primary influences on the ^{207}Pb chemical shift so that ^{207}Pb NMR may be developed as a structural probe for lead local environments in disordered materials of complex composition.

Experimental Section

Most of the crystalline samples were high purity (Merck 99.9%) obtained commercially and checked by powder X-ray diffraction (XRD). The exceptions were the lead silicate phases, PbSiO_3 and $\text{H-Pb}_2\text{SiO}_4$, which were synthesized by a previously described sol-gel process with lead nitrate and tetraethoxysilane precursors.³

The ^{207}Pb NMR experiments were carried out on Bruker MSL and DSX 300 spectrometers (7.0 T) operating at 62.6 MHz for ^{207}Pb , using standard 4 and 7 mm MAS probes (Bruker). Magic angle spinning (MAS) spectra were obtained with spinning rates from 1 to 15 kHz, using single pulse ($\pi/9$) acquisition. Static ^{207}Pb NMR spectra were collected with use of a Hahn echo sequence ($\pi/2-\tau-\pi-\tau$ -acquire). The pulse length was varied from 2.7 μs to 0.6 μs to verify complete irradiation of the spectra. The recycle delay between acquisitions was varied from a few seconds to a few minutes to ensure no saturation. The number of acquisitions ranged from 32, for narrow spectra (typically $\text{Pb}(\text{NO}_3)_2$), to 32 000, when intensity was spread over numerous spinning sidebands. Chemical shifts were referenced to tetramethyllead $\text{Pb}(\text{CH}_3)_4$ at 0 ppm, using a 0.5 M aqueous lead nitrate solution as a secondary reference⁴ ($\delta = -2941$ ppm vs $\text{Pb}(\text{CH}_3)_4$). All spinning experiments were carried out at nominally room temperature, but some spectra did exhibit slight shifts related to spinning speed, which we attributed to an increase of temperature inside the MAS rotor due to frictional heating. The high sensitivity of solid state ^{207}Pb chemical shift to changes in temperature has been reported already for lead nitrate.^{5,6}

The processing of these ^{207}Pb spectra with extensive spinning sideband manifolds was carried out very carefully, ensuring that all Fourier transforms started at $t = 0$ (probe deadtime at 62.6 MHz was typically 8 μs). Otherwise, problems with the phase of the sidebands can lead to spectra that are difficult to interpret.⁷ Sometimes three or four spectra of the same sample at different spinning speeds were required in order to unambiguously assign the isotropic bands.

The intensities of spinning sidebands were fitted to obtain the associated chemical shift anisotropies with a modified version of the WINFIT program⁸ (Bruker) according to Herzfeld and Berger.⁹ The

(3) Bessada, C.; Massiot, D.; Coutures, J.; Douy, A.; Coutures, J. P.; Taulelle, F. *J. Non-Cryst. Solids* **1994**, *168*, 76–85.

(4) Irwin, A. D.; Chandler, C. D.; Assink, R.; Hampden-Smith, M. J. *Inorg. Chem.* **1994**, *33*, 1005–1106.

(5) Sebald, A. *NMR* **1994**, *31*, 91–131.

(6) Van Gorkom, L. M. C.; Hook, J. M.; Logan, M. B.; Hanna, J. V.; Wasylishen, R. E. *Magn. Reson. Chem.* **1995**, *33*, 791–795.

(7) Yoko, T.; Kiyoharu, K.; Miyaji, F.; Sakka, S. *J. Non-Cryst. Solids* **1992**, *150*, 192–196.

[†]Present address: Department of Earth Sciences, University of Cambridge, Downing Street, Cambridge CB2 3EQ, UK.

[⊗] Abstract published in *Advance ACS Abstracts*, July 1, 1997.

(1) Kim, K. S.; Bray, P. J. *J. Magn. Reson.* **1974**, *16*, 334–338.

(2) Piette, L. H.; Weaver, H. E. *J. Chem. Phys.* **1958**, *28*, 735.

Table 1. ²⁰⁷Pb Chemical Shifts of the Lead-Containing Compounds^a

| compd | δ_{iso} (ppm) ^b | Ω (ppm) | K | δ_{11} (ppm) | δ_{22} (ppm) | δ_{33} (ppm) |
|---|--|----------------|-------|---------------------|---------------------|---------------------|
| Pb(NO ₃) ₂ | -3494 ± 2 (-3491.6 ¹⁵) | 55 | 1 | -3475.6 | -3475.6 | -3530.6 |
| PbCO ₃ | -2630 ± 2 (-2622.4 ¹⁵) | 793 | 0.6 | -2312.8 | -2471.4 | -3105.8 |
| PbSO ₄ | -3613 ± 2 (-3505 ¹⁵) | 563.5 | 0.43 | -3371.6 | -3532.5 | -3935.1 |
| PbMoO ₄ | -2009 ± 2 (-2004.9 ¹⁵) | 182 | -1 | -1887.7 | -2069.6 | -2069.6 |
| Pb ₃ (PO ₄) ₂ : Pb(1) | -2886 ± 2 | 210 | -0.64 | -2758.6 | -2930.8 | -2968.6 |
| Pb(2) | -2016 ± 2 | 1784 | 0.64 | -1314.3 | -1635.4 | -3098.3 |
| PbCl ₂ | -1717 ± 2 (-1723 ⁷) | 533 | 0.64 | -1507.3 | -1603.3 | -2040.3 |
| PbF ₂ | -2667 ± 2 (-2668 ¹⁴) | 443 | 0.53 | -2484.6 | -2588.7 | -2927.6 |
| red PbO | 1939 ± 5 | 3114 | 1 | 2977 | 2977 | -137 |
| yellow PbO | 1515 ± 5 | 3917 | 0.81 | 2944.7 | 2572.6 | -972.3 |
| Pb ₃ O ₄ : Pb ⁴⁺ | -1105 ± 1 | 158 | -0.69 | -1007.8 | -1141.3 | -1165.8 |
| Pb ²⁺ | 795 ± 2 | 3048 | 0.69 | 1968.5 | 1496 | -1079.5 |
| PbSiO ₃ : Pb(1) | 93 ± 5 | 2878 | 0.66 | 1215.4 | 726.1 | -1662.6 |
| Pb(2) | -166 ± 5 | 3259 | 0.69 | 1088.7 | 583.6 | -2170.3 |
| Pb(3) | -366 ± 5 | 3061 | 0.64 | 838 | 287 | -2223 |
| H-Pb ₂ SiO ₄ : Pb(3) | 329 ± 5 | 3579 | 0.75 | 1671.1 | 1223.7 | -1907.8 |
| Pb(1) | 634 ± 5 | 3602 | 0.81 | 1948.7 | 1606.5 | -1653.2 |
| Pb(4) | 1344 ± 5 | 3712 | 0.81 | 2698.9 | 2346.2 | -1013.1 |
| Pb(2) | 1382 ± 5 | 3824 | 0.87 | 2739.5 | 2491 | -1084.5 |

^a The uncertainties for δ_{CSA} vary from ±3 ppm for lower range up to ±15 ppm for higher values, $\eta_{\text{CSA}} \pm 0.05$. ^b Chemical shift is referenced relative to Pb(CH₃)₄.

Table 2. Crystallographic Data of the Lead Containing Compounds

| compd | space group | Z/unit cell | cell dimens (nm) | Pb ²⁺ coord no. | Pb-X mean bond length (nm) |
|---|---------------------------|-------------|---|--|--|
| Pb(NO ₃) ₂ ³³ | <i>P3a</i> | 4 | $a = 0.7859$ | 12 | $\bar{d}(\text{Pb-O}) = 0.2809$ |
| PbCO ₃ ³³ | <i>Pbnm</i> | 4 | $a = 0.8468, b = 0.6146, c = 0.5166$ | 9 (6 + 3) | $\bar{d}(\text{Pb-O}) = 0.2702$ |
| PbSO ₄ ³⁴ | <i>Pnma</i> | 4 | $a = 0.8480, b = 0.5398, c = 0.6958$ | 12 | $\bar{d}(\text{Pb-O}) = 0.2889$ |
| PbMoO ₄ ²⁵ | <i>I4₁/a</i> | 4 | $a = 0.5435, c = 1.2108$ | 8 | $\bar{d}(\text{Pb-O}) = 0.2657$ |
| Pb ₃ (PO ₄) ₂ ³⁵ | <i>C2/c</i> | 4 | $a = 1.3816, b = 0.5692, c = 0.9429, \beta = 102^\circ 36'$ | Pb(1): 6 Pb(2): 7 | $\bar{d}(\text{Pb-O}) = 0.2660$ $\bar{d}(\text{Pb-O}) = 0.2658$ |
| PbCl ₂ ³⁶ | <i>Pbnm</i> | 4 | $a = 0.9030, b = 0.7608, c = 0.4525$ | 7 | $\bar{d}(\text{Pb-Cl}) = 0.2986$ |
| PbF ₂ ³⁶ | <i>Pbnm</i> | 4 | $a = 0.7636, b = 0.6427, c = 0.3891$ | 9 | $\bar{d}(\text{Pb-F}) = 0.2652$ |
| red PbO ³⁷ | <i>P4/nmm</i> | 2 | $a = 0.396, c = 0.501$ | 4 | $\bar{d}(\text{Pb-O}) = 0.2309$ |
| yellow PbO ³⁸ | <i>Pbcm</i> | 4 | $a = 0.5893, b = 0.5490, c = 0.4753$ | 4 | $\bar{d}(\text{Pb-O}) = 0.2358$ |
| Pb ₃ O ₄ ¹⁷ | <i>P4₂/mbc</i> | 4 | $a = 0.8811, c = 0.6563$ | Pb ⁴⁺ : 6 Pb ²⁺ : 4 | $\bar{d}(\text{Pb-O}) = 0.2176$ $\bar{d}(\text{Pb-O}) = 0.2374$ |
| PbSiO ₃ ¹⁸ | <i>P2/n</i> | 12 | $a = 1.123, b = 0.708, c = 1.226, \beta = 113^\circ 25'$ | Pb(1): 3 Pb(2): 4 Pb(3): 4 | $\bar{d}(\text{Pb1-O}) = 0.2389$ $\bar{d}(\text{Pb2-O}) = 0.2356$ $\bar{d}(\text{Pb3-O}) = 0.2416$ |
| H-Pb ₂ SiO ₄ ¹⁹ | <i>A12/m</i> | 32 | $a = 3.8789, b = 0.7567, c = 1.2212, \beta = 96^\circ 78'$ | Pb(3): 3 Pb(1): 3 Pb(4): 3 Pb(2): 3 | $\bar{d}(\text{Pb3-O}) = 0.2382$ $\bar{d}(\text{Pb1-O}) = 0.2216$ $\bar{d}(\text{Pb4-O}) = 0.2270$ $\bar{d}(\text{Pb4-O}) = 0.2249$ |

chemical shift anisotropy (CSA) can be characterized by the following three parameters:¹⁰ the isotropic chemical shift, δ_{iso} , the span, Ω , which measures the full extend of the spectrum, and the skew, K , the deviation from cylindrical symmetry. Here, these parameters are defined according to the following conventions:¹⁰

$$\delta_{\text{iso}} = \frac{1}{3}(\delta_{11} + \delta_{22} + \delta_{33})$$

$$\Omega = \delta_{11} - \delta_{33} \geq 0$$

$$K = \frac{3(\delta_{22} - \delta_{\text{iso}})}{\Omega} \quad (1)$$

with the principal components defined in the sequence:

- (8) Massiot, D.; Thiele, H.; Germanus, A. *Bruker Rep.* **1994**, *140*, 43-46.
 (9) Herzfeld, J.; Berger, A. E. *J. Chem. Phys.* **1980**, *73*, 12, 6021-6030.
 (10) Mason, J. *Solid. State NMR* **1993**, *2*, 285-288.

$$\delta_{11} \geq \delta_{22} \geq \delta_{33} \quad (2)$$

Results

The ²⁰⁷Pb NMR chemical shifts of the lead-containing compounds studied in this work are reported in Table 1, and the crystallographic data for each crystal form are reported in Table 2. Figure 1 shows the spectrum of PbSO₄ and is typical of ionic lead compounds with a single site ($\delta_{\text{iso}} = -3613$ ppm, $\Omega = 563.5$ ppm, $K = 0.43$). For these ionic compounds, the ²⁰⁷Pb chemical shifts range approximately between -3700 and -1000 ppm. The ²⁰⁷Pb shifts measured in MAS experiments are in good agreement with previous static NMR studies¹¹⁻¹⁵

- (11) Nolle, A. Z. *Naturforsch.* **1977**, *32a*, 964-967.
 (12) Lutz, O.; Nolle, A. Z. *Phys.* **1980**, *B36*, 323-328.
 (13) Nizam, M.; Allavena, M.; Bouteiller, Y. *J. Magn. Reson.* **1989**, *82*, 441-453.
 (14) Neue, G.; Dybowski, C.; Smith, M. L.; Barich, D. H. *Solid. State NMR* **1994**, *3*, 115-119.

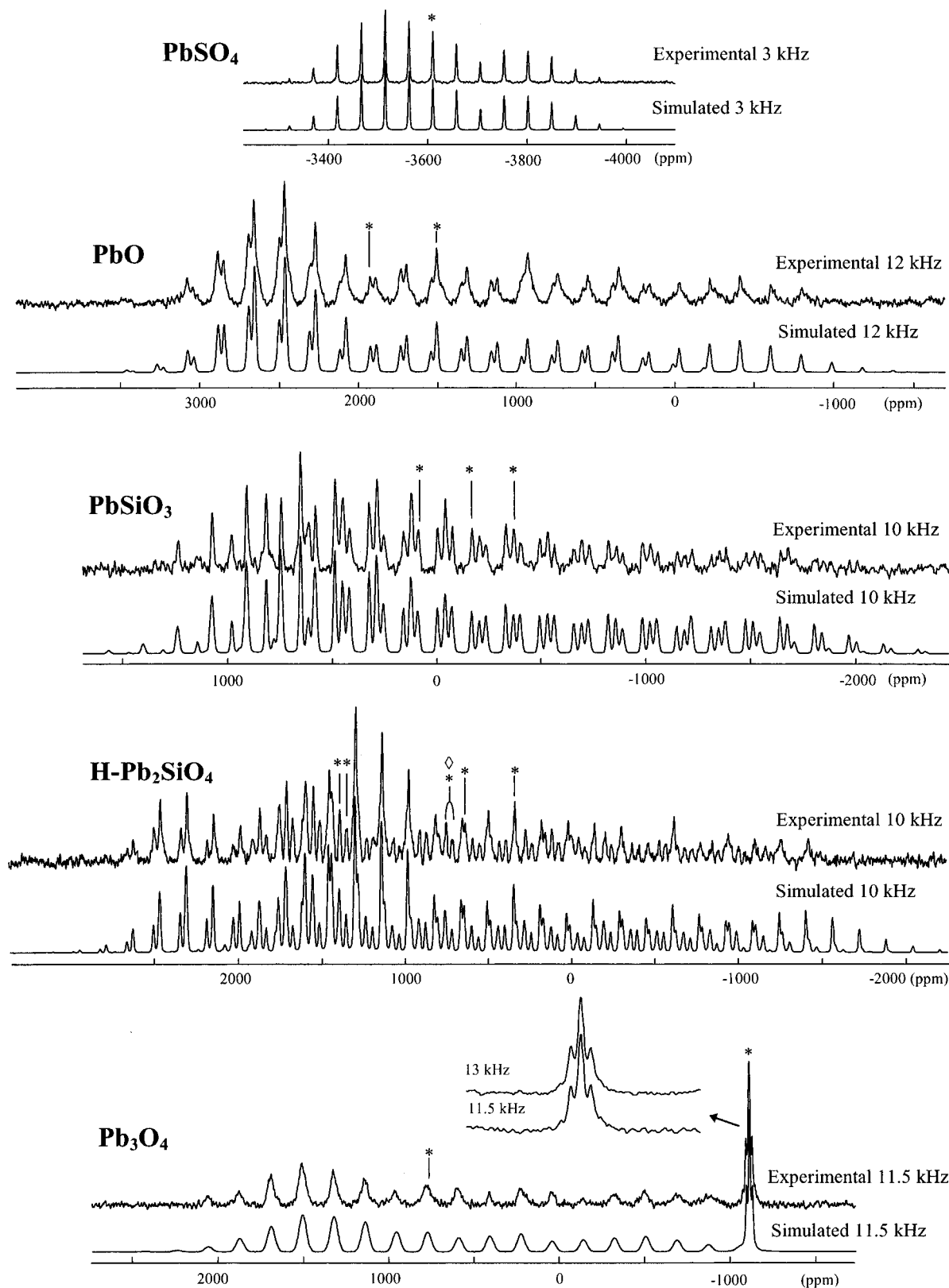


Figure 1. ^{207}Pb MAS NMR spectra of PbSO_4 , PbO , PbSiO_3 , $\text{H-Pb}_2\text{SiO}_4$, and Pb_3O_4 (asterisks mark isotropic lines, \diamond indicates impurity).

for $\text{Pb}(\text{NO}_3)_2$, PbCO_3 , PbMoO_4 , PbCl_2 , and PbF_2 but differ by some 110 ppm for PbSO_4 (Table 1). We have carefully rechecked this shift and also examined the published spectrum in ref 15 to find that the discrepancy is not a typing error. More covalent compounds such as PbO give positive chemical shifts with larger spinning sideband manifolds among which isotropic

shifts are more difficult to determine. The assignments in these cases are detailed below.

The spectrum of lead monoxide (PbO) is shown in Figure 1. PbO exists in two polymorphic forms. Red PbO (Litharge) is tetragonal and yellow PbO (Massicot) is orthorhombic; both phases contain single lead sites. The ^{207}Pb MAS NMR spectra of PbO (Figure 1) clearly show the presence of both of these two phases which exhibit large chemical shift anisotropies and

(15) Neue, G.; Dybowski, C.; Smith, M. L.; Hepp, M. A.; Perry, D. L. *Solid State NMR* **1996**, *6*, 241–250.

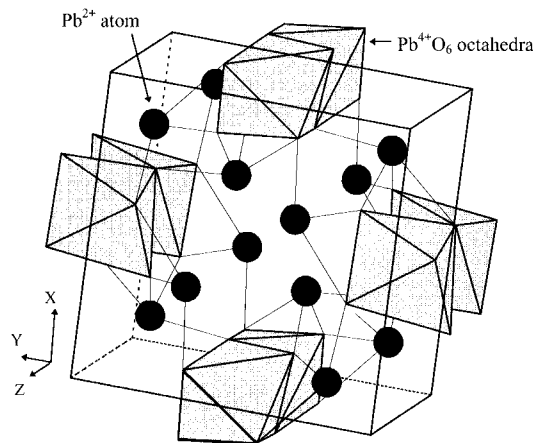


Figure 2. View of the unit cell of Pb_3O_4 .

integrated intensities in the ratio 3:1, in agreement with X-ray diffraction analysis. The most intense contribution ($\delta_{\text{iso}} = 1515$ ppm, $\Omega = 3917$ ppm, $K = 0.81$) is attributed to yellow PbO , and the second spinning sideband pattern, centered at 1939 ppm, with an axially symmetric CSA tensor ($\Omega = 3114$ ppm, $K = 1$), is attributed to the red tetragonal form. The spectra at two spinning speeds were required to determine the isotropic chemical shifts, and the CSA tensor parameters were fitted to match the two spectra. Both phases have layered structures containing infinite Pb-O chains. The Pb^{2+} atoms are located on the surface of the sheets and are bonded to four oxygens, forming a square pyramid with a lead atom at the apex. The layers are then bonded together by Van der Waals interactions between the electronic lone pair of Pb^{2+} atom.¹⁶ Pb-O bond lengths are shorter than the sum of ionic radii (0.26 nm), indicating a highly covalent character for the Pb-O bond.¹⁶ In the tetragonal form, the Pb-O bond lengths and bond angles are the same, whereas in yellow PbO , the PbO_4 square pyramids are severely distorted. The distinction between red and yellow resonances can be made on the basis of signal intensity and the smaller span and skew of the Pb axially symmetric site in the tetragonal form ($K = 1$).

The crystalline network of Pb_3O_4 (Minium) consists of chains of PbO_6 octahedra (the octahedra are joined by sharing two edges) linked by square PbO_4 pyramids.¹⁷ In the tetragonal phase (room temperature), there are two lead valences and two different coordinations. Two-thirds of the lead atoms are Pb^{2+} in a pyramidal coordination and the others are Pb^{4+} in octahedral coordination. Figure 1 shows the MAS spectrum of Pb_3O_4 : two distinct contributions are observed with integrated intensities in the ratio 2:1. The spectrum consists of a large manifold of sidebands, similar to that in PbO , centered at 795 ppm, assigned to the Pb^{2+} site and a narrow symmetric line ($\delta_{\text{iso}} = -1105$ ppm) corresponding to the Pb^{4+} ionic site, associated with two symmetric satellites having a spinning rate independent separation. These satellites are attributed to the J coupling between the Pb^{4+} and a neighboring lead site populated by a ^{207}Pb atom ($J = 2260$ Hz). In the Pb_3O_4 structure, the Pb^{4+} site has two Pb^{4+} closest neighbors at a distance of 0.328 nm (Figure 2). Considering the natural abundance of ^{207}Pb (22.5%) and the possible site occupancies (isolated ^{207}Pb , pair or triplet), this results in a multiplet that we clearly observe in Figure 1. The calculated intensities are $62.5:(2 \times 17.4):(2 \times 1.25)$ for the center band and the first and second pair of satellites, respectively. The measured intensities are $59.2:(2 \times 17.8):(2 \times 2.6)$; however, a spinning sideband from Pb^{2+} overlaps the narrow

J -coupled line interfering with the measured intensities. Note that J coupling is not resolved on the Pb^{2+} spectrum. The intrinsic line width of the Pb^{4+} resonance is much less than that for Pb^{2+} , and the possibilities of chemical shift dispersion due to the pyramidal geometry probably serve to obscure J coupling in this case. The low chemical shift anisotropy of the octahedral site has been measured from a static spectrum.

The ^{207}Pb MAS NMR spectrum of Alamosite (PbSiO_3) shows three sets of spinning sidebands corresponding to the three Pb sites present in the unit cell (Figure 1). The structure consists of zigzag chains of SiO_4 tetrahedra perpendicular to screw chains of PbO_4 and PbO_3 pyramids.¹⁸ The crystalline network is made up of these two types of chains linked together by Pb-O-Si bonds. In the lead-oxygen spiral chains, two types of Pb are in the form of PbO_4 square pyramids and another Pb atom forms PbO_3 trigonal pyramids. The short interatomic distances between lead and oxygen indicate the covalent character of these Pb-O bonds. The two isotropic peaks at -366 and -166 ppm can be attributed to Pb in PbO_4 pyramids ($\text{Pb}(2)$ and $\text{Pb}(3)$) with the remaining peak at 93 ppm attributed to Pb in a trigonal pyramid (site $\text{Pb}(1)$). Considering that a decrease in mean Pb-O bond length is associated with a more positive chemical shift in lead monoxide, the isotropic peak at -166 ppm might be assigned to the site labeled $\text{Pb}(2)$ with the shorter mean PbO bond length.

Lead orthosilicate (Pb_2SiO_4) has four different polymorphic phases, but only the structure of $\text{H-Pb}_2\text{SiO}_4$ (the higher temperature phase) has been determined by X-ray diffraction.¹⁹ Our sample was checked by powder XRD to correspond to the $\text{H-Pb}_2\text{SiO}_4$ described by Katto.¹⁹ However, examination of the XRD pattern also has shown the presence of an impurity identified as the $\text{M-Pb}_2\text{SiO}_4$ phase. According to Katto, the complex structure of this lead silicate consists of Si_4O_{12} rings and ribbons of PbO_3 trigonal pyramids. In this description, there are four unequivalent Pb sites in the unit cell. Two of them involve only Pb-O-Pb bonds while the other sites involve Pb-O-Si bonds. As shown on Figure 1, the ^{207}Pb MAS spectrum of this sample is extremely complex and exhibits six isotropic peaks at 1382, 1344, 745, 710, 634, and 329 ppm, each with large spinning sideband manifolds. These six isotropic peaks correspond to six unequivalent Pb sites that we can try to link to the four sites of $\text{H-Pb}_2\text{SiO}_4$ described by Katto. By using Katto's description of the structure, the two peaks at 1382 and 1344 ppm (close to the yellow PbO value) should correspond to the sites with Pb-O-Pb linkages ($\text{Pb}(2)$, $\text{Pb}(4)$). As previously, the assignment of the line with more positive chemical shift is made by considering its shorter mean Pb-O bond lengths. The other four peaks would then appear to correspond to PbO_3 units with silicon neighbors (Pb-O-Si bonds) as described by Katto (Pb bound via oxygen to two silicon atoms). The two peaks with highest intensity at 329 and 634 ppm might be assigned to the $\text{Pb}(3)$ and $\text{Pb}(1)$ sites, while the contributions with lowest intensities and highest chemical shift values (744, 710 ppm) might be attributed to traces of the $\text{M-Pb}_2\text{SiO}_4$ phase (distorted PbO_3 pyramidal unit close to the $\text{Pb}(1)$ site).

Discussion

Structural Correlations. In order to use NMR chemical shifts as a structural probe, it is necessary to establish the relationship between them and the different local environments of atoms in different structures. First principles calculations of chemical shifts are possible, but the precision to which shifts

(16) Dickens, B. *J. Inorg. Nucl. Chem.* **1965**, *27*, 1495–1501.

(17) Gavarrí, J. R.; Weigel, D. *J. Solid State Chem.* **1975**, *13*, 252–257.

(18) Boucher, M. L.; Peacor, D. R. *Z. Krist.* **1968**, *126*, 98–111.

(19) Katto, K. *Acta Crystallogr.* **1980**, *B36*, 2539–2545.

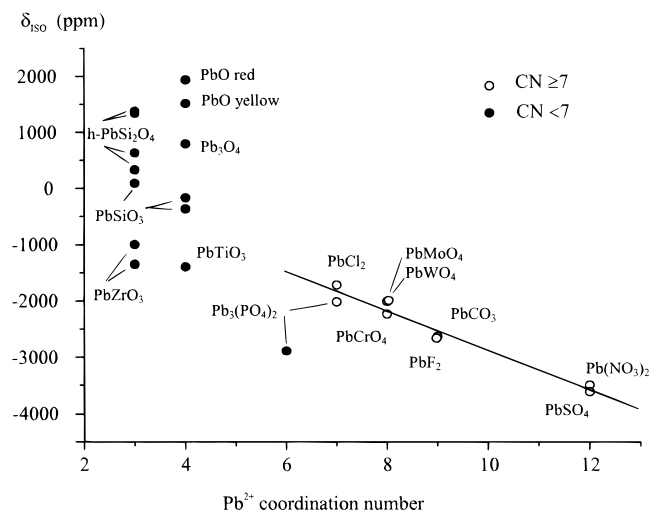


Figure 3. Evolution of $\delta_{\text{iso}}^{207\text{Pb}}$ vs Pb coordination number (the straight line gives the linear correlation for $\text{CN} \geq 7$: $R = 0.979$, $n = 9$, δ_{iso} (ppm) = $622.8 - 349.7\text{CN}$).

can be measured in NMR exceeds that of the calculations, although the rank ordering of the shifts of different structures can be derived from calculation.²⁰ The general approach is to establish an empirical correlation by measuring shifts of materials of known structure.

The magnetic shielding, σ , of a nucleus occurs because of the modified motion of its surrounding electrons induced by the applied external magnetic field. There are two effects: a diamagnetic induced field due to the circulation of electrons in the core which opposes the applied external field and a second paramagnetic field due to a slight unquenching of orbital angular momentum in electron orbitals with orbital angular momentum.²¹ The shielding is, thus, generally written as the contribution of two terms:²² $\sigma = \sigma_{\text{dia}} + \sigma_{\text{para}}$, where σ_{dia} is the diamagnetic term and σ_{para} the paramagnetic term. In the case of heavy nuclei like Pb, the variation of the σ_{para} contribution is dominant but very difficult to evaluate by formal computation.

We used a simplified approach to understanding shift/structure correlations for the ^{207}Pb chemical shifts in oxides and silicates, and we propose to establish correlations between NMR experimental parameters and simple structural parameters that will allow structural information to be determined from ^{207}Pb NMR spectra of unknown structures.

For nuclei such as ^{29}Si or ^{27}Al , the structural change responsible for the major changes in NMR chemical shift is local coordination change.²³ Figure 3 shows the influence of this parameter on the ^{207}Pb chemical shift for the Pb compounds examined. Additional NMR^{4,11,15} and crystallographic data^{24–27} from the literature for PbWO_4 , PbCrO_4 , PbTiO_3 , and PbZrO_3 have also been plotted here. The data plotted as a function of coordination number are in general agreement for coordination being a controlling parameter for chemical shifts, at least for coordination numbers of seven and over. The general evolution of ^{207}Pb shifts vs Pb coordination number shows that as the

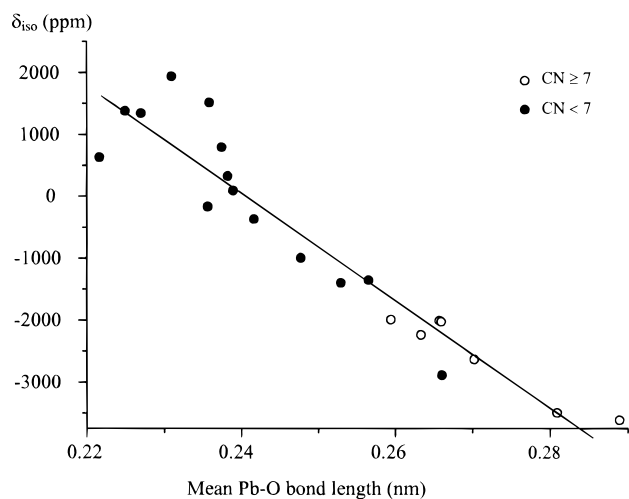


Figure 4. Evolution of $\delta_{\text{iso}}^{207\text{Pb}}$ vs mean Pb–O bond length (the straight line gives the linear correlation: $R = 0.953$, $n = 21$, δ_{iso} (ppm) = $20854 - 86689.5d(\text{Pb–O})$ (nm)).

coordination number decreases, the paramagnetic shielding increases (chemical shift more positive). If we look at just the lead coordinations of seven or greater (Figure 3), then a reasonable correlation for shift vs coordination is found with $R = 0.979$ and $n = 9$:

$$\delta_{\text{iso}} \text{ (ppm)} = 622.8 - 349.7\text{CN} \quad (3)$$

If we restrict the lead first neighbors to be oxygens and look at the correlation between the mean Pb–O bond length (varying from 0.2216 to 0.2889 nm) and chemical shift (Figure 4), a good correlation is found with $R = 0.953$ and $n = 21$:

$$\delta_{\text{iso}} \text{ (ppm)} = 20854 - 86689.5d(\text{Pb–O}) \text{ nm} \quad (4)$$

Considering the large variations of lead local environment for the compounds studied, the mean Pb–O bond length appears to be a reasonable controlling parameter for Pb^{2+} chemical shifts, even if the departure from linearity increases for the more covalent compounds with short mean bond length. Considering the empirical eq 4, as the mean bond length decreases the paramagnetic shielding increases (negative slope) leading to more positive chemical shift, and a bond length variation of 0.001 nm should correspond to a shift difference of about 86.7 ppm. If we look at just the lead coordinations of seven or greater, the correlation coefficient is slightly improved ($R = 0.957$, $n = 7$: δ_{iso} (ppm) = $14836 - 64323.4d(\text{Pb–O})$ nm).

For the more ionic compounds, the similar good correlations between coordination number and mean bond length are not surprising since steric effects will mean that coordination number and bond length are themselves highly correlated for a single ligand type.

Covalent Compounds. For the more covalent lead compounds, such as lead oxides and silicates, simple chemical shift–structure relationships based on coordination number and mean Pb–O bond lengths give poor correlation coefficients ($R < 0.6$, $n = 9$). In these materials lead usually has a pyramidal, 3- or 4-fold coordination with oxygen. However, the general trends of the influence of coordination number on the shift are still true. Chemical shifts for three- and four-coordinated lead are more positive than higher coordinations (see Figure 3). The chemical shift range for these lower coordinations becomes larger and causes the ranges of 3- and 4-fold coordination to overlap almost completely. The large range of shifts for these coordinations means that it should be possible to derive further

(20) Tossel, J. A. *Phys. Chem. Miner.* **1984**, *10*, 137–141.

(21) Slichter, C. P. *Principles of Magnetic Resonance*, 3rd ed.; Springer-Verlag: Berlin, 1990; pp 87–108.

(22) Pople, J. A. *Proc. R. Soc.* **1957**, *A239*, 541–549.

(23) Engelhardt, G.; Michel, D. *High-resolution solid-state NMR of silicates and zeolites*; John Wiley and Sons: Chichester, 1985; pp 122–134.

(24) Effenberger, H.; Pertlik, F. *Z. Krist.* **1986**, *176*, 75–83.

(25) Sleight, A. W. *Acta Crystallogr.* **1972**, *B28*, 2899–2902.

(26) Shirane, G.; Pepinsky, R.; Frazer, B. C. *Acta Crystallogr.* **1956**, *9*, 131.

(27) Jona, F.; Shirane, G.; Mazzi, F.; Pepinsky, R. *Phys. Rev.* **1957**, *105*, 849–856.

structural information by relating the shifts to other more subtle structural parameters.

One such parameter could be the bond angles at the lead site such as is used to correlate ^{29}Si chemical shifts in silicates when Si is tetrahedrally coordinated by oxygen in sp^3 hybridization. In the case of Si, linear correlations have been proposed with use of mean bond angle,²⁸ but using these for Pb, in lead oxides and silicates, yields poor correlation coefficients ($R < 0.6$, $n = 9$). The best empirical correlation has been obtained by relating the bond angles to the degree of s-hybridization of the oxygen orbitals. This formulation has been used successfully to reproduce trends in ^{29}Si chemical shifts in silicates and aluminosilicates.^{29,30} The degree of s-hybridization, ρ , of the oxygen (sp^n hybridization, $1 \leq n \leq 3$) is given by the equation:²⁹

$$\rho = (\cos \theta)/(\cos \theta - 1) \quad (5)$$

where θ is the Pb–O–Pb bond angle. For an asymmetric Pb–O–X linkage the oxygen atomic orbitals in the PbO and XO bonds are inequivalent and will be characterized by different degrees of s-hybridization. To a first approximation, this difference between cation electronegativities may be taken into account by using an empirical corrective factor³⁰ that is proportional to the number of unsymmetric linkages. We have applied this formulation to lead oxides and silicates by considering $\text{Pb}(\text{OPb})_{m-n}(\text{OSi})_n$ units and the following modified equation:

$$P = [(\cos \theta)/(\cos \theta - 1)] + AN \quad (6)$$

where θ is the mean Pb–O–X bond angle ($X = \text{Pb}$ or Si), N is the number of Si atoms bound via oxygen to the lead atom, and A is a constant to take into account the electronegativity difference between Si and Pb. A good correlation is obtained by using the reliable data of PbSiO_3 (3 sites) the two PbO polymorphs and taking $A = 0.2$. A least-squares fit gives the following correlation ($R = 0.982$ with $n = 5$):

$$\delta_{\text{iso}} \text{ (ppm)} = 2306.4 - 2395.7P \quad (7)$$

When, following the analysis of the data for $\text{H-Pb}_2\text{SiO}_4$, we added the four assigned sites to the additional five sites with Pb–O–(Pb/Si) linkages, the data fell satisfyingly close to the line and this linear correlation is confirmed ($R = 0.969$ with $n = 9$):

$$\delta_{\text{iso}} \text{ (ppm)} = 2076.2 - 2180.2P \quad (8)$$

This plot is shown in Figure 5, and the values of eq 7 are given in Table 3. In this correlation, we used a corrective term A close to the electronegativity difference between Pb and Si,³¹ but this constant is of rather low weight to the linearity of the correlation. In these lead oxides and lead silicates, constituted of PbO_m pyramidal units ($m = 3, 4$), the mean Pb–O–X bond angles are between 108° and 120° , $((\cos \theta)/(\cos \theta - 1))$ between 0.24 and 0.34. With use of the value $A = 0.2$, the term AN , which corrects for the modified degree of s-hybridization due to Si rather than Pb neighbors, is of the same order of magnitude as the $(\cos \theta)/(\cos \theta - 1)$ term, and both the increase of the Pb–O–X angle and the addition of Si into the second coordination sphere of Pb cause the ^{207}Pb chemical shift to

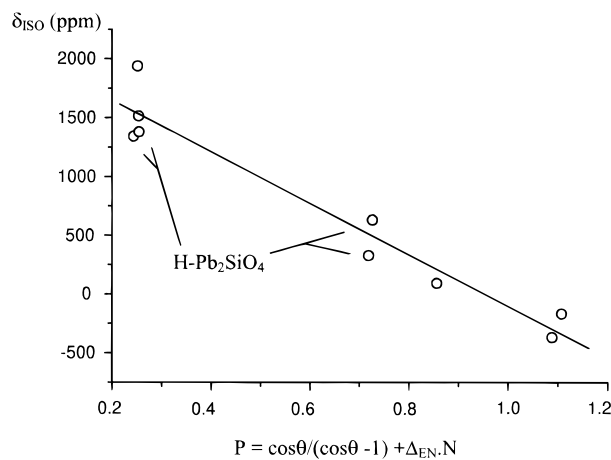


Figure 5. Evolution of $\delta_{\text{iso}}^{207}\text{Pb}$ vs P parameter (the straight line gives the linear correlation: $R = 0.969$, $n = 9$, $A = 0.2$, $\delta_{\text{iso}} \text{ (ppm)} = 2076.2 - 2180.2P$).

Table 3. Mean Pb–O–X Bond Angle, Number of Si in the Pb Second Coordination Sphere ($N(\text{Si})$), and Degree of s-Hybridization of the Oxygen (P) for the Crystalline Lead Oxides and Silicates

| compd | Pb–O–X mean bond angle (deg) | $N(\text{Si})$ | P |
|-------------------------------------|------------------------------|----------------|-------|
| red PbO | 109.6 | 0 | 0.251 |
| yellow PbO | 109.8 | 0 | 0.253 |
| PbSiO_3 : Pb(1) | 110.2 | 3 | 0.856 |
| Pb(2) | 116.3 | 4 | 1.107 |
| Pb(3) | 113.9 | 4 | 1.088 |
| $\text{H-Pb}_2\text{SiO}_4$: Pb(1) | 118.9 | 2 | 0.726 |
| Pb(2) | 109.9 | 0 | 0.254 |
| Pb(3) | 117.8 | 2 | 0.718 |
| Pb(4) | 108.7 | 0 | 0.243 |

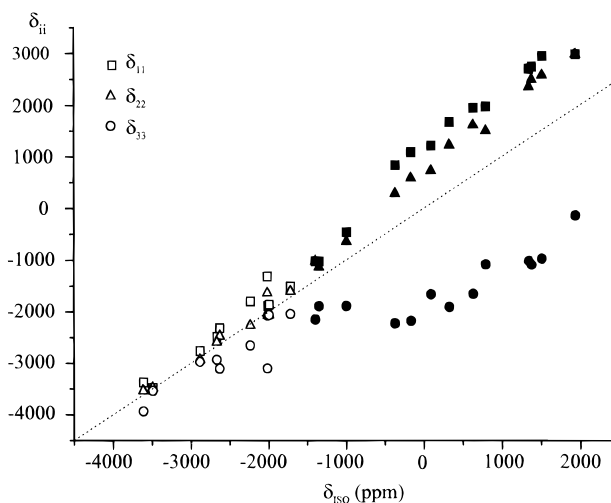


Figure 6. Evolution of the principal components of the CSA tensor vs the isotropic shift.

become more negative. The explanation for ^{207}Pb chemical shifts to decrease with increasing Pb–O–X mean bond angle would be similar to that for silicates: increasing the degree of s-hybridization (ρ increasing) causes the p character to diminish and the paramagnetic contribution to the chemical shift to fall and shifts are more negative for higher bond angles.

Chemical Shift Anisotropy. Since the chemical shift anisotropy (CSA) is caused by the nonspherical symmetry of the bonding environment around the nucleus, empirical correlations between anisotropy and structure generally use an average deviation of bond angles (O–X–O) or bond lengths from that of a perfect polyhedron (XO_n).³² These typical

(28) Ramdas, S.; Klinowski, J. *Nature* **1984**, *308*, 521.

(29) Engelhardt, G.; Radeglia, R. *Chem. Phys. Lett.* **1984**, *108*, 3, 271–274.

(30) Radeglia, R.; Engelhardt, G. *Chem. Phys. Lett.* **1985**, *114*, 1, 28–30.

(31) Gordy, W.; Thomas, W. J. O. *J. Chem. Phys.* **1956**, *24*, 2, 439–444.

correlations yield poor results in the case of Pb. However, the large spans of ^{207}Pb NMR spectra show its sensitivity to slight deviations from spherical symmetry. Figure 6 shows the evolution of the principal components of the CSA tensor versus the isotropic shift of Pb^{2+} . For the ionic compounds, the isotropic and principal values of the CSA tensor are of the same order of magnitude. For the covalent Pb bonding state (lead oxides and silicates), we observe a large splitting between δ_{33} and $\delta_{11} \approx \delta_{22}$, interpreted as being due to the steric effect of the electronic lone pair of Pb^{2+} which prevents the existence of symmetric environments with short Pb–O bond lengths. For the covalent compounds, the lead atoms occupy the apex of a distorted pyramidal PbO_n unit ($n = 3, 4$). This gives a close to axial symmetry shielding tensor ($\delta_{11} \approx \delta_{22}$, $|\text{K}| \approx 1$) where δ_{33} is approximately along the symmetry axis (lone pair).

Conclusion

^{207}Pb magic angle spinning NMR can provide reliable isotropic chemical shifts when care is taken to unambiguously

(32) Turner, G. L.; Smith, K. A.; Kirkpatrick, R. J.; Olfield, E. *J. Magn. Reson.* **1986**, *70*, 408–415.

(33) Wyckoff, R. W. G. *Crystal Structures* 2nd ed.; Interscience: New York, 1960; Vol. 2.

(34) Wyckoff, R. W. G. *Crystal Structures*, 2nd ed.; Krieger, R. E., Ed.: Malabar, 1981; Vol. 3.

(35) Keppler, U. Z. *Krist.* **1970**, *132*, 228–235.

(36) Wyckoff, R. W. G. *Crystal Structures*; Interscience: New York, 1960; Vol. 1.

assign spectra that consist of manifolds of sidebands often overlapping in a complex manner. These can be assigned to different lead sites in crystalline lead oxides and lead silicates and used to derive empirical correlations between ^{207}Pb isotropic chemical shifts and structural parameters. We have established experimentally the following primary influences on Pb^{2+} chemical shifts. For ionic compounds, we observe good linear correlations between chemical shift and Pb^{2+} coordination number or mean Pb–O bond length. For more covalent compounds, the best empirical correlation has been obtained by using the degree of s-hybridization of the oxygen and the relative electronegativity of dissimilar second neighbors. These correlations, established for simple crystalline compounds, should allow the use of ^{207}Pb NMR as a structural probe for lead local environments in disordered materials of complex composition.

Acknowledgment. This work was supported by Centre de Recherches et d'Essais pour l'Environnement et le Déchet (CREED), CNRS (UP 4212), and Région Centre. The authors thank A. Douy for sol-gel synthesis and M. P. Faugere for providing commercial samples. The authors also thank the referees for constructive remarks on the manuscript.

JA963593F

(37) Leciejewicz, J. *Acta Crystallogr.* **1961**, *14*, 1304.

(38) Hill, R. J. *Acta Crystallogr.* **1985**, *C41*, 1281–1284.